

Reductive Functionalization of Carbon Nanotubes

F. Borondics, M. Bokor, P. Matus, K. Tompa, and S. Pekker
Research Institute for Solid State Physics and Optics, Budapest, Hungary

E. Jakab
Chemical Research Center, Budapest, Hungary

Abstract: We present sidewall functionalization of carbon nanotubes via various dissolving metal reduction methods. Carbanion complexes of lithium were prepared in liquid ammonia and THF and reacted with a series of alkyl and aryl halogenides, as well as methanol resulting in the formations of alkylated, arylated, and hydrogenated nanotube derivatives, respectively. The hydrogenation reactions were also performed on graphite. Thermal stabilities and chemical compositions were determined by thermogravimetry-mass spectrometry (TG-MS). Characteristic decomposition peaks, observed in the range of 350–600°C, suggest the formation of covalent derivatives upon functionalization. The compositions are 0.01–0.25 side group/carbon depending on the materials. NMR and Raman spectroscopic characterizations show the structural changes due to functionalization.

Keywords: Functionalization of nanotubes, thermal stability, hydrogenation, alkylation

INTRODUCTION

Functionalization of carbon nanotubes is an effective way to enhance the physical properties and improve the solubility, however, the aromatic character of nanotubes restricts the possible addition reactions. Various functionalization methods have been carried out such as fluorination (1, 2), oxidation (3), Birch reduction (4, 5), direct addition of reactive organic

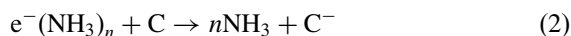
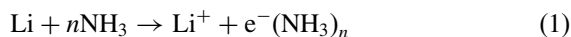
Address correspondence to F. Borondics, Research Institute for Solid State Physics and Optics, HAS, P.O. Box 49, Budapest H-1525, Hungary. E-mail: pekker@szfki.hu

molecules (4, 6–9), and modifications of the primary functional groups (10, 11). The latter methods, especially amidation and esterification of sidewall carboxylic groups are generally used for the attachment of various functional groups. A few recent reviews summarize the most important reactions (12–14).

Here we describe a novel dissolving metal reduction method of functionalization. Previously, hydrogenation of graphite and nanotubes were carried out by Birch reduction in liquid ammonia (5). We extended this method to alkylation and arylation, and besides the use of NH_3 solvent, we performed the reactions in THF with lithium naphthalenide. The compositions, thermal stabilities, and structural characterizations of the functionalized materials are discussed.

FUNCTIONALIZATION

Carbonaceous materials were hydrogenated and functionalized via various dissolving metal reduction methods with lithium in liquid ammonia and/or tetrahydrofuran (THF). Powdered graphite (Johnson Matthey, ultra carbon) and bucky paper of single-walled carbon nanotubes (SWNTs, Tubes@Rice) were annealed in vacuum at 800°C and stored in a glove box prior to use. Ammonia was distilled from lithium while THF from potassium benzophenone. Other reagent grade materials were used as purchased from Aldrich. Hydrogenation of graphite and SWNTs in NH_3 was performed via a Birch-reduction method described previously (5). Briefly, 20 mL dried NH_3 was condensed to the mixture of 50 mg carbon and 150 mg Li and stirred for an hour at about -50°C . Then, 20 mL methanol was added to the reactants. After the solvent became colorless, the reaction mixture was heated to ambient temperature, washed subsequently with methanol, water, dilute hydrochloric acid, water and methanol, and dried in vacuum at ambient temperature. The first steps of the proposed hydrogenation reactions are the solution of lithium in ammonia and the formation of its carbanion complex:

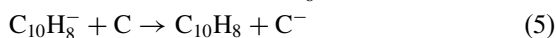
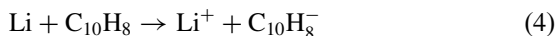


In a subsequent step methanol decomposes the carbanion forming the hydrogenated carbon derivative:



In THF, the reduction was performed with the radical anion salt of lithium naphthalenide. Typically 50 mg C, 150 mg Li, and 4 g naphthalene were suspended in 40 mL THF. The deep green solution was stirred for an hour.

The analogous reactions of Eqs. (1) and (2) are:



The carbanion was decomposed via Eq. (3) and the product was processed as before. To remove naphthalene, the material was also washed with toluene.

Alkylation and arylation of SWNTs were performed in both NH_3 and THF, similarly to hydrogenation. The carbanion was decomposed with alkyl or aryl halogenides:



where RX = methyl iodide, butyl iodide, and benzyl bromide. Alkyl and aryl halogenides were dissolved in ether or THF and used in large excess ($20\times$) to decrease the influence of the direct reaction with the reducing agents.

COMPOSITION AND THERMAL STABILITY

The chemical composition and the thermal stability of the samples were studied by thermogravimetry-mass spectrometry (TG-MS). The TG-MS instrument consists of a Perkin–Elmer TGS-2 thermobalance and a HIDEN HAL 2/301 PIC quadrupole mass spectrometer. Typically 2–4 mg samples were heated at a $20^\circ\text{C}/\text{min}$ heating rate from 30°C to 800°C in argon atmosphere. A portion of the volatile products was introduced into the mass spectrometer operating at 70 eV in electron impact ionization mode. The intensities of 16 selected ions were monitored together with the thermogravimetric parameters.

We did not observe any mass loss or volatile product formation from pristine graphite or SWNT samples. The prepared materials contained large amounts of solvents, therefore, the hydrogenated samples were heat treated at 350°C for 3 hr, while the less stable alkylated and arylated samples were kept at 200°C for 12 hr. The TG-MS curves of all functionalized materials show decomposition steps characteristic of the side groups and the preparation method. The MS intensity profiles of the expected decomposition products describe the major features of the DTG curves. Supporting previous results (5), hydrogenated derivatives decompose in the $400\text{--}600^\circ\text{C}$ range with maximum rates at $T_{\text{max}} = 500^\circ\text{C}$. The major decomposition product is hydrogen accompanied with a smaller amount of methane.

The decomposition of alkyl and aryl derivatives of SWNTs is more complex, however, still characteristic of single phase materials. Three overlapping steps can be observed at 350, 500 and 600°C . The maximum decomposition rates of all materials are at about $T_{\text{max}} = 350^\circ\text{C}$. Fig. 1. shows the TG-MS curves of methylated SWNTs, prepared in liquid NH_3 .

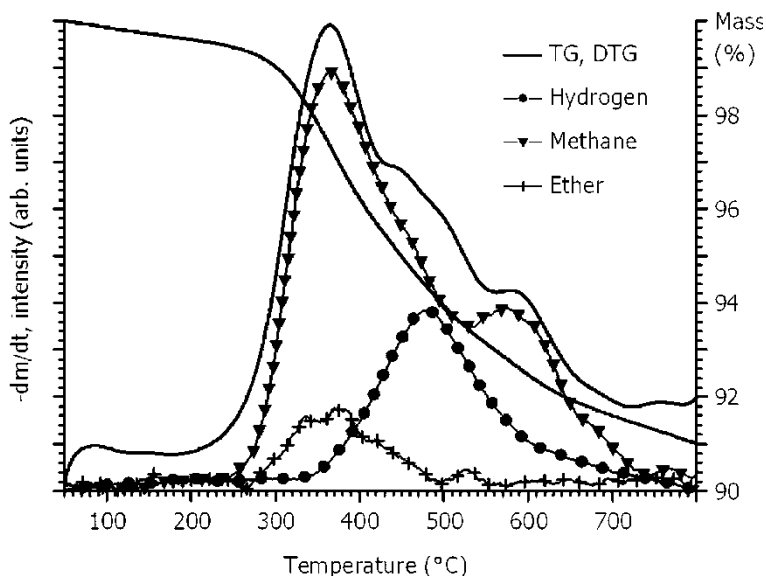


Figure 1. Thermal decomposition of methylated SWNTs, prepared in liquid NH_3 : thermogravimetric curves (TG, DTG) and the evolution profiles of methane (m/z 16), hydrogen (m/z 2), and diethyl ether (m/z 59).

The evolution profiles of methane (m/z 16) and hydrogen (m/z 2) follow the shape of DTG curve. The only volatile impurity is diethyl ether (m/z 59), which was the solvent of methyl iodide. Its high evolution temperature indicates a strong interaction, probably a condensation inside the tubes during the methylation reaction. The H_2 evolution profile strongly resembles those of hydrogenated samples. Similar dehydrogenation can be observed in all materials upon heating, especially in those prepared in liquid NH_3 , indicating a competing hydrogenation reaction during functionalization. The second methane peak of smaller intensity at 600°C can also be observed in all materials including hydrogenated derivatives and may be attributed to the decomposition of CH groups (5).

Fig. 2 shows the decomposition of butylated SWNTs, prepared in THF. Here butane (m/z 43) is the major decomposition product and the characteristic decomposition temperatures are similar to those of the methylated derivative.

The chemical compositions of the functionalized materials are summarized in Table 1. In most cases the composition was calculated from the mass loss corresponding to the temperature region of the major decomposition peaks. Due to the parallel evolution of impurities this method overestimates the amount of functional groups and may give rise to significant error for

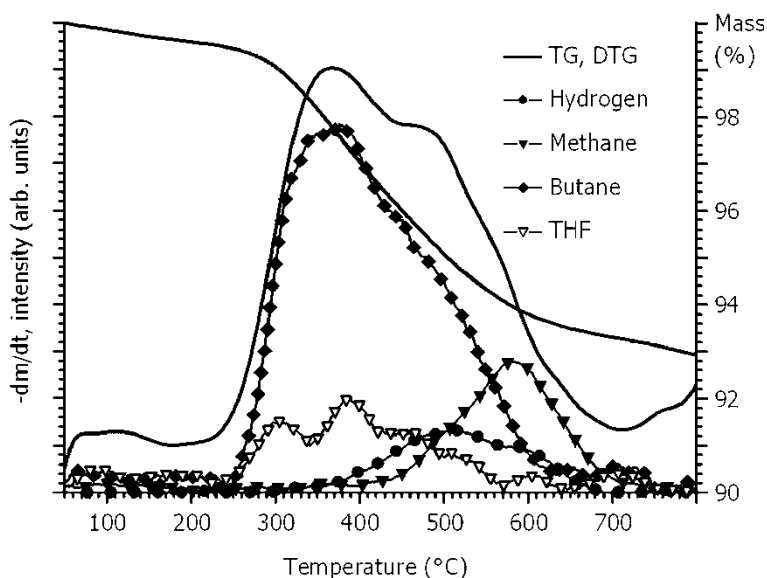


Figure 2. Thermal decomposition of butylated SWNTs, prepared in THF: thermogravimetric curves (TG, DTG), and the evolution profiles of butane (m/z 43) hydrogen (m/z 2), methane (m/z 16), and THF (m/z 72).

hydrogen of low molar mass. To eliminate this error, the mass spectrometer was calibrated for hydrogen by using the thermal decomposition of TiH_2 and the hydrogen yield was calculated from the MS data. As shown in Table 1, the H content of graphite derivative prepared in NH_3 is as high as 26 mol%, corresponding to about a C_4H stoichiometry. Much less H content can be achieved in THF. On the other hand, the THF method proved to be effective for the functionalization of SWNTs with large

Table 1. Composition and thermal stability of functionalized carbon samples

Side group	Carbon	Solvent	$\Delta G(\%)$	H/100C (MS)	H/100C (NMR)	R/100C (TG)	T_{max} ($^{\circ}C$)
H	Graphite	NH_3	5.3	26	20		500
H	Graphite	THF	3.2	1.2			500
H	SWNT	NH_3	5.3	3.2	2.5		500
Methyl	SWNT	NH_3	8.0	2.0		6.4	350
Methyl	SWNT	THF	6.2	0.6		5.0	350
Butyl	SWNT	NH_3	8.4	1.6		1.8	350
Butyl	SWNT	THF	6.3	0.6		1.3	350
Benzyl	SWNT	NH_3	8.7	1.0		1.1	350

functional groups. This method has an increased importance when the large organic molecules have lower solubility in NH_3 .

STRUCTURAL CHARACTERIZATION

Hydrogenated graphite and SWNTs were characterized by solid-state ^1H -NMR spectroscopy. ^1H -NMR measurements were accomplished by a Bruker SXP 4–100 pulse spectrometer of $\sim 10^{-6}$ resolution at 82.57 MHz frequency. Echo signals were generated by the pulse sequence $X-\tau-Y$ ($\tau = 30 \mu\text{s}$). Spectra, normalized to unit amplitude are shown in Fig. 3. The linewidth of the hydrogenated graphite spectrum (fwhm = 16 ppm) is characteristic of immobile hydrogen with an average H—H distance of 0.28 nm. Assuming uniformly distributed H atoms in the graphite lattice, this value is in good qualitative agreement with the hydrogen contents obtained from both the peak integral of the same NMR spectrum (C_5H) and the TG/MS results (C_4H). The very broad spectrum of the hydrogenated SWNTs (fwhm = 590 ppm) compared to graphite is due to the residual magnetic catalyst particles. Only a poor estimate of lower limit of 1 H atom per 40 C atoms could be given for the bound hydrogen content of the SWNTs because of the strong influence of the catalyst residues.

Raman spectra were recorded using a Renishaw System 1000B spectrometer equipped with a microscope. For the measurements we used a

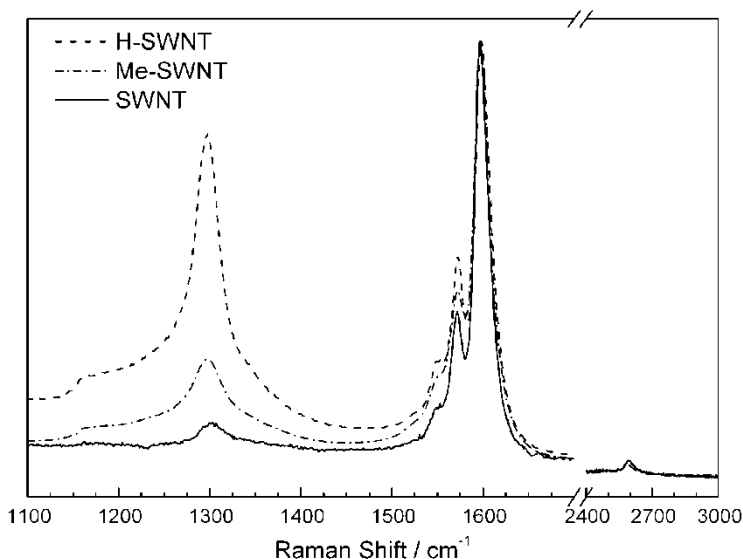


Figure 3. Normalized ^1H -NMR spectra of hydrogenated graphite and SWNTs.

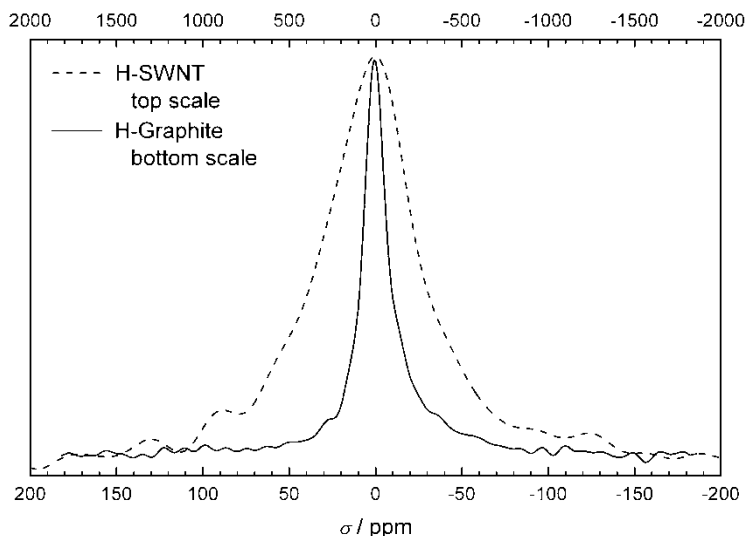


Figure 4. Raman spectra of functionalized and pristine SWNTs, normalized to the G band.

diode laser operated at 785 nm with approximately 500 μW power on sample. Spectra were recorded in the 200–3000 cm^{-1} range. The influence of hydrogenation and methylation on the Raman spectrum of SWNTs is displayed in Fig. 4. The most significant change is the increase of the intensity of the D band at around 1300 cm^{-1} . Since this peak is attributed to the scattering on defects i.e., on sp^3 carbons in the sp^2 system, its increase supports the formation of C–H and C–C bonds due to hydrogenation or methylation. On the other hand, the high intensity of the resonant scattering of the nanotubes prevented the detection of CH stretching modes.

CONCLUSION

We have prepared hydrogenated, alkylated, and arylated derivatives of SWNTs and hydrogenated graphite by dissolving metal reductions in liquid ammonia and THF. The high thermal stability and the sharp, characteristic decomposition curves measured by TG-MS suggest the formation of covalent C–C and C–H bonds due to functionalization.

The covalent structure is supported by the increased intensity of the Raman line at 1300 cm^{-1} . The hydrogenation of graphite in NH_3 resulted in the formation of a high hydrogen content derivative, with C_4H composition. The NMR linewidth corresponds to immobile, strongly bound hydrogen.

Further experimental evidence is needed to reveal the local bonding nature of hydrogen in graphite. The functional group contents of SWNTs are in the range of 1–6 mol%, depending on the material and the method applied. A significant amount of hydrogen can be observed in all materials functionalized in NH₃, indicating a competing hydrogenation reaction. Further alkylation and arylation reactions and the detailed structural characterization of the formed materials are in progress.

ACKNOWLEDGMENT

This work was supported by the grants OTKA: T032613, T037704, and T046700.

REFERENCES

1. Hamwi, A., Alvergnat, H., Bonnamy, S., and Beguin, F. (1997) *Carbon*, 35: 723.
2. Mickelson, E.T., Huffman, C.B., Rinzler, A.G., Smally, R.E., Hauge, R.H., and Margrave, J.L. (1998) *Chem. Phys. Lett.*, 296: 188.
3. Mawhinney, D.B., Naumenko, V., Kuznetsova, A., Yates, J.T., Jr., Liu, J., and Smally, R.E. (2000) *J. Am. Chem. Soc.*, 122: 2383.
4. Chen, Y., Haddon, R.C., Fang, S., Rao, A.M., Eklund, P.C., Lee, W.H., Dickey, E.C., Grulke, E.A., Pendergrass, J.C., Chavan, A., Haley, B.E., and Smalley, R.E. (1998) *J. Mater. Res.*, 13: 2423.
5. Pekker, S., Salvetat, J.-P., Jakab, E., Bonard, J.-M., and Forró, L. (2001) *J. Phys. Chem. B*, 105: 7938.
6. Bahr, J.L. and Tour, J.M. (2001) *Chem. Mater.*, 13: 3823.
7. Georgakilas, V., Kordatos, K., Prato, M., Guldi, D.M., Holzinger, M., and Hirsch, A. (2002) *J. Am. Chem. Soc.*, 124: 760.
8. Hu, H., Zhao, B., Kamaras, K., Itkis, M.E., and Haddon, R.C. (2003) *J. Am. Chem. Soc.*, 125: 14893.
9. Tagmatarchis, N. and Prato, M. (2004) *J. Mater. Chem.*, 14: 437.
10. Sun, Y.-P., Huang, W., Lin, Y., Fu, K., Kitaygorodskiy, A., Riddle, L.A., Yu, Y.J., and Carroll, D.E. (2001) *Chem. Mater.*, 13: 2864.
11. Huang, W., Lin, Y.L., Taylor, S., Gaillard, J., Rao, A.M., and Sun, Y.-P. (2002) *Nano Lett.*, 2: 231.
12. Niyogi, S., Hamon, A., Hu, H., Zhao, B., Bhowmik, P., Sen, R., Itkis, M.E., and Haddon, R.C. (2002) *Acc. Chem. Res.*, 35: 1105.
13. Hirsch, A. (2002) *Angew. Chem. Int. Ed.*, 41: 1853.
14. Seo, J.W., Couteau, E., Umek, P., Hernadi, K., Marcoux, P., Lukic, B., Mikó, Cs., Milas, M., Gaál, R., and Forró, L. (2003) *New J. Phys.*, 5: 120.